Investigating Sorption on Iron−Oxyhydroxide Soil Minerals by Solid-State NMR Spectroscopy: A ^{6}Li MAS NMR Study of Adsorption and Absorption on Goethite

Ulla Gro Nielsen,[†,‡] Younkee Paik,[†,‡,§] Keinia Julmis,[†,‡] Martin A. A. Schoonen,[‡,||] Richard J. Reeder,[‡,||] and Clare P. Grey*[,†,‡]

Department of Chemistry, Department of Geosciences, and Center for Environmental Molecular Science, State University of New York at Stony Brook, Stony Brook, New York 11794-2275

Received: March 18, 2005; In Final Form: July 14, 2005

High-resolution ^{2}H MAS NMR spectra can be obtained for nanocrystalline particles of goethite (α-FeOOH, particle size ≈ 4−10 nm) at room temperature, facilitating NMR studies of sorption under environmentally relevant conditions. Li sorption was investigated as a function of pH, the system representing an ideal model system for NMR studies. ^{6}Li resonances with large hyperfine shifts (approximately 145 ppm) were observed above the goethite point of zero charge, providing clear evidence for the presence of Li−O−Fe connectivities, and thus the formation of an inner sphere Li^+ complex on the goethite surface. Even larger Li hyperfine shifts (289 ppm) were observed for Li^+-exchanged goethite, which contains lithium ions in the tunnels of the goethite structure, confirming the Li assignment of the 145 ppm Li resonance to the surface sites.

Introduction

Goethite (α-FeOOH), an iron oxyhydroxide, is one of the most common inorganic soil minerals and is formed in aqueous environment at ambient temperatures. Its strong uptake capacity for toxic metals[1,2] and (hazardous) oxyanions[3−6] render it an important sorbent for toxic ions in the environment. The diversity in chemical composition, as well as the structural and physical properties of natural samples, can be reproduced in the laboratory by controlling the synthetic conditions.[7−11] Thus, goethite serves as a useful model compound for studies of ion sorption on inorganic soil minerals.

Numerous experimental studies have shown that the surface properties of goethite, especially the reactivity of different surface O−H groups, are important in determining mobility, reversibility, and the fate of sorbed species. Microscopy, along with various surface spectroscopic techniques, has been used to investigate the structures of the surface complexes, and the capacity, kinetics, and mechanisms of ion uptake, as a function of the environmental conditions (e.g., pH).[1,2,4,12,13] Semiempirical models, such as the multisite complexation (MUSIC) model, have been developed to help rationalize these results and predict surface properties and uptake behavior of goethite and other minerals. These have utilized molecular-level information, such as the charge of the metal ions, bond connectivity, and distances between metal and oxygen atoms, as well as the strengths of hydrogen bonding in the structure.[14,15]

Goethite has orthorhombic symmetry (*Pbnm*, space group No. 62) and is isostructural to groutite (α-MnOOH) and diaspore (α-AlOOH).[16] It consists of edge-sharing FeO_6 octahedra connected to form distorted rectangular-shaped "2 × 1" tunnels (i.e., tunnels that are 2 FeO_6 × 1 FeO_6 octahedra in diameter) along the *c* axis (Figure 1). Two hydrogen atoms are asymmetrically bonded across the tunnel to two oxygen atoms. The magnetic structures of the different goethites have been studied extensively by Mössbauer spectroscopy,[17,22] neutron diffraction,[23] low- and high-field susceptibility measurements,[18,24] and positron annihilation lifetime spectroscopy.[21] Goethite is an antiferromagnet below its Néel transition temperature (T_N) of approximately 130 °C and is paramagnetic above it.[17−19] However, T_N depends strongly on the extent of cation doping, the particle size, and the concentrations of vacancies or defects, dropping to below room temperature for nanoparticles of goethite.[19,20]

Characterization of sorption on soil minerals such as goethite is challenging due to, for example, the disordered and often complex structure of the surface, the possibility of surface reconstruction, and the mobility of sorbed species on the surface. Moreover, species may sorb simultaneously at multiple sites, with different coordination geometries. In principle, NMR spectroscopy represents an ideal method for probing the structure of ions or molecules bound on surfaces. However, NMR spectroscopic studies of this class of minerals are extremely challenging due to the presence of unpaired electron spins on the Fe^{3+} ions, which interact strongly with any nuclear spins in their vicinity. Liquid-state, ^{133}Cs longitudinal relaxation (T_1) times have been used to probe Cs^+ interactions with the surface of iron minerals,[25] but no high-resolution, solid-state NMR studies have, to our knowledge, been reported. We have recently demonstrated that high-resolution solid-state ^{2}H NMR spectra can be obtained for the paramagnetic phase of goethite, suggesting that it may be possible to use NMR spectroscopy to study sorption on iron oxides and hydroxides with T_N values near room temperature,[26] as long as the T_1 relaxation times of the electron spins are fast in the NMR time scale, as found in our earlier studies of goethite, vanadates, and manganates[26−28] and magnetic properties are carefully controlled.

* Corresponding author. Fax: 1-631-632-5731. E-mail: cgrey@notes.cc.sunysb.edu.
[†] Department of Chemistry.
[‡] Center for Environmental Molecular Science.
[§] Current address: Department of Chemistry, Washington University, Saint Louis, MO 63130.
[||] Department of Geosciences.

10.1021/jp051433x CCC: $30.25
Published on Web 09/13/2005

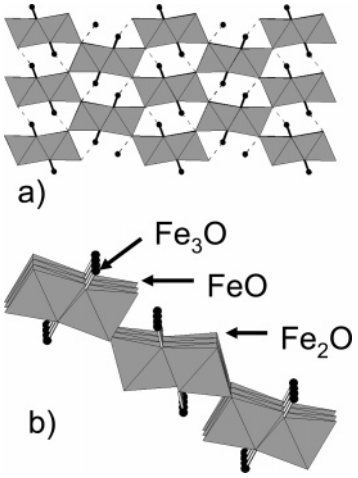

Figure 1. (a) Structure of goethite (space group *Pbnm*)[16] viewed along the *c* axis, and (b) the predominant (110) surface. FeO, Fe_2O, and Fe_3O indicate the positions of surface oxygen atoms coordinated to one, two, and three iron atoms, respectively (see text). The actual number of hydrogen atoms attached to each surface group is highly pH-dependent.

As an initial feasibility study, we chose to investigate lithium sorption on goethite, as a function of pH, with ^{6}Li MAS NMR spectroscopy. Li^+ was used as a model ion for small cations such as Mg^{2+}, since a wide range of lithium-containing paramagnetic materials have been studied by ^{6}Li/^{7}Li NMR. Furthermore, the large hyperfine (or Fermi-contact) shifts in these systems have been shown to reflect the Li local environments and the number and angles of M−O−Li connectivities, where M^{n+} is a metal ion such as Mn^{4+}.[29] ^{6}Li (7.4% natural abundance, $\gamma = 3.9 \times 10^7$ rad·T^{-1}·s^{-1}, eQ $= -8 \times 10^{-4}$ barn) was used instead of ^{7}Li NMR, since ^{6}Li has a lower gyromagnetic ratio (γ) and smaller quadrupole moment (eQ) than ^{7}Li (92.6% natural abundance, $\gamma = 10.4 \times 10^7$ rad·T^{-1}·s^{-1}, eQ $= -4 \times 10^{-2}$ barn). The lower γ of ^{6}Li attenuates the strong dipolar interaction between Li and the unpaired electrons by a factor of 2.5 and results in fewer spinning sidebands in MAS experiments. For similar reasons, we employ ^{2}H instead of ^{1}H NMR to study the (pristine) goethite.[26] In addition, problems with the significant ^{1}H background in the experimental equipment are circumvented.

We demonstrate in this paper that Li sorption on goethite can be probed by solid-state ^{2}H and ^{6}Li MAS NMR spectroscopy under environmentally realistic conditions, by using a sample containing nanoparticles of goethite, with a Néel transition below room temperature. The results are compared with those for $^6Li^+$-exchanged goethite, so as to distinguish signals obtained from Li^+ sorbed in the goethite tunnels with those due to Li^+ on the surfaces. H^+ for Li^+ ion exchange is possible since Li^+ is sufficiently small to fit in the tunnels formed by the iron oxide framework.

Experimental Section

Synthesis. *Goethite.* Nanoparticles of goethite, "nano-goethite or n-α-FeOOH", were synthesized following the method of Goodman and Lewis.[30] A 500 mL aliquot of 0.02 M iron(II) chloride (98%, Aldrich) solution was treated with sodium bicarbonate (Fisher), in an excess of 5 mM, to raise the pH and buffer the solution near pH 7 during the subsequent oxidation. Air was bubbled through the solution at room temperature at a constant rate of 20−25 mL/min for 48 h. The color of the suspension changed from pale green, to a darker green, to yellow-brown, as the oxidation progressed. Deuterated nanoparticles of goethite (n-α-FeOOD) were prepared in D_2O (98%, Cambridge Isotope Laboratories) using the same procedure as described above. The products were washed free of salt by repeated washing (4−5 times). The product was isolated by centrifugation and subsequently freeze-dried. All samples were characterized by X-ray diffraction.

Li^+ Adsorption. Nanocrystalline goethite (1 mg/mL) was suspended in 50 mM solution of $^6Li^+$, prepared from ^{6}LiOH·H_2O to produce two series of samples. The pH was then adjusted by adding 1 M nitric acid. The Li-sorbed goethite was isolated after 48 h by centrifugation and subsequently dried in air for a few days. No efforts to exclude CO_2 from the solutions were made. Series A consisted of five samples with Li^+ sorbed at pH = 4.0, 6.1, 7.4, 9.5, and 11.1 (samples 4.0A, 6.1A, 7.4A, 9.5A, 11.1A), while series B consisted of three samples with Li^+ sorption at pH = 4.0, 9.3, and 11.1, respectively (sample 4.0B, 9.3B, and 11.1B).

Li^+-Exchanged α-FeOOH. This compound was prepared by an ion-exchange reaction of micrometer-sized goethite (m-α-FeOOH) following the procedure of Sakurai et al.[31] A 0.079 g amount of lithium hydroxide monohydrate (^{6}LiOH·H_2O, 90−95% ^{6}Li, Cambridge Isotope Laboratories) was dissolved in 11 mL of 2-phenoxyethanol and 0.190 mg of goethite was added. The suspension was heated to 190 °C for 4 h in a thermostatically controlled oil bath, after which the sample was isolated and washed with ethanol. m-α-FeOOH was synthesized following the procedure of Schwertmann et al,[7] as recently described in detail.[26] Our attempts to ion-exchange nanocrystalline goethite failed under these reaction conditions. This is most likely due to the conversion of the goethite to hematite at the high reaction temperatures used in this procedure, the conversion to hematite proceeding more quickly and/or at a lower temperature for the smaller particle materials.

Characterization. Powder X-ray diffraction data of n-α-FeOOH and n-α-FeOOD were collected on a Scintag powder X-ray diffractometer (Cu Kα radiation). BET surface areas for these samples were measured on a Micromeritics ASAP 2010 gas sorption analyzer using N_2. The point of zero charge (PZC) and particle size distribution were determined by using a ZetaPlus light scattering device equipped with both dynamic phase analysis light scattering (PZC measurements)[32,33] and dynamic light scattering (particle size), Brookhaven Instruments Corp. Scanning electron microscopy (SEM) and transmission electron microscopy (TEM) images were obtained on Leo 1550 and Philips CM12 machines, respectively. Particle sizes were estimated visually from these images.

^{2}H and ^{6}Li MAS NMR experiments were performed at 30.73 and 29.45 MHz, respectively, on a CMX-200 spectrometer with a Chemagnetics 4 mm MAS probe. Spectra were recorded by employing a rotor-synchronized Hahn-echo pulse sequence, with evolution time periods of one rotor period. Values of $\gamma B_1 \approx 90$ kHz, 500 kHz spectral windows, 0.2 s relaxation delays, and spinning speeds of 14−17 kHz were used. ^{2}H and ^{6}Li NMR spectra were referenced relative to D_2O ($\delta_{iso} = 4.8$ ppm) and 1 M ^{6}LiCl ($\delta_{iso} = 0$ ppm), respectively.

Results and Discussion

A detailed description of the physical properties of the different goethite samples used for ion-exchange experiments is first given, which is followed by the results from the ^{6}Li MAS NMR study of Li^+sorption on goethite. Finally, the characterization of Li^+-exchanged, micrometer-sized α-FeOOH with variable temperature (VT) ^{6}Li MAS NMR is presented.

Diffraction, Surface Area Determination, and SEM/TEM of Nano-Goethite. Powder X-ray diffraction (XRD) of both

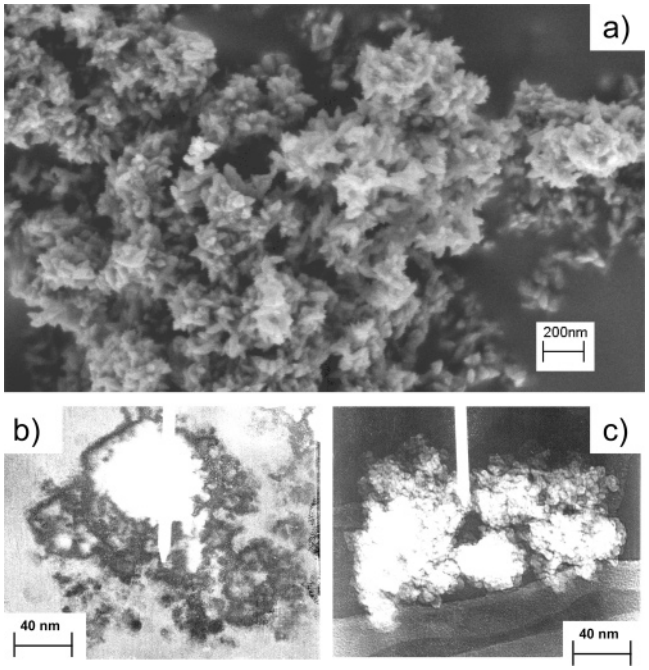

Figure 2. (a) Scanning electron microscopy (SEM) and (b) tunneling electron microscopy (TEM) images of a nanocrystalline deuterated goethite (n-α-FeOOD). (c) TEM image of a nanocrystalline hydrogen form of goethite (n-α-FeOOH).

the protonated and deuterated nano-goethite samples (n-α-FeOOH/D) showed fairly broad peaks, indicating a small particle size and/or low crystallinity of the sample. However, the diffraction pattern could be unambiguously indexed on the basis of the crystal structure reported in the literature (space group *Pbnm*).[8] Debye Scherrer analysis of the peak widths gave an estimate of ≈6 nm, for the particle sizes. BET surface areas of 219.8 (±0.6) and 228.7 (±0.7) m^2/g were measured for hydrogen and deuterium forms of n-α-FeOOH, respectively.

The SEM and TEM images of both the unlabeled and deuterated forms of the synthetic goethite crystals, obtained to investigate the particle size distribution and sample morphology, show mainly nanosize particles (4−10 nm in diameter) agglomerated into clumps of particles 0.1−1 μm in diameter (Figure 2). A bimodal particle size distribution of 0.10−0.13 μm (20% of all particles) and 0.5−1.0 μm (80%) was obtained from the light scattering measurements. The smaller particles are consistent with the clusters of nanoparticles observed in the TEM and SEM images, while the larger particles are either due to further agglomeration and/or the presence of larger particles of goethite, which were missed in the TEM/SEM images.

^{2}H MAS NMR Spectra of Goethite. High-resolution ^{2}H MAS NMR spectra were obtained for the n-α-FeOOD samples even at room temperature, as illustrated in Figure 3a. Very similar spectra are recorded at 100 and 150 °C (Figure 3b,c). The results should be contrasted with our previous ^{2}H MAS NMR study of micron sized goethite (m-α-FeOOD),[26] where a broad featureless spectrum was seen at room temperature. A sharp signal was only observed above the Néel transition temperature of this sample (≈120−130 °C). Thus, the Néel Temperature (T_N) for the antiferro- to paramagnetic phase for nano-crystalline goethite has dropped to below room temperature.[26] The suppression of T_N by more than 100 K is presumably due to the small particle size, as previously suggested.[19] The spectra are characteristic of a rigid OD bond, in agreement with the crystal structure of goethite. They

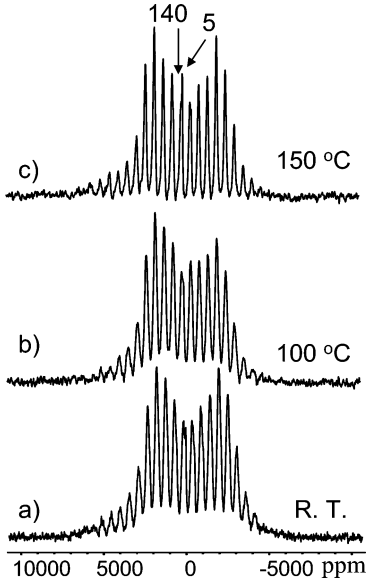

Figure 3. Variable-temperature ^{2}H MAS NMR spectra of deuterated nanocrystalline goethite (n-α-FeOOD) recorded at (a) room temperature, (b) 100 °C, and (c) 150 °C. The isotropic shift for n-α-FeOOD is at 140 ppm; the resonance at 5 ppm most likely originates from surface water.

can be simulated using the 208 kHz quadrupole coupling constant extracted from the ^{2}H MAS NMR spectrum of m-α-FeOOD.[26]

A more detailed analysis of the spectra in Figure 3 shows that the high-resolution resonance is superimposed on a broader resonance, the latter disappearing at 150 °C and above. This broad resonance constitutes approximately 5−15% of the total signal intensity based on an integration of the ^{2}H MAS NMR spectrum. This indicates that the n-α-FeOOD sample contains a subset of particles with Néel temperatures of ≈100−150 °C, closer to the T_N values seen for micrometer-sized goethite particles. This result is consistent with the light scattering experiment, where larger particles were observed in addition to the nanoparticles.

The large observed isotropic shift (140 ppm) is ascribed to the Fermi contact (hyperfine) shift mechanism, which is caused by a transfer of unpaired electron density from the Fe^{3+} ions (d^5, $S = {}^5/_2$) to the 1s orbital on the ^{2}H atoms and is proportional to the susceptibility (χ).[28,34] No discernible changes of the isotropic shift are observed by increasing the temperature. This implies an essentially constant value of χ in this temperature regime, presumably due to strong residual antiferromagnetic (AF) couplings between the iron (electron) spins, even above T_N. This is consistent with magnetic susceptibility measurements for goethites, which typically show a poorly defined T_N and only small changes in χ above T_N.[17] Quite broad isotropic resonances and spinning sidebands (≈7 kHz), which do not narrow significantly at higher temperatures, are observed for n-α-FeOOD, compared to the line widths previously seen for m-α-FeOOD (1 kHz above 150 °C). The broadening is ascribed to a distribution of local environments for the deuterons, leading to a range of hyperfine shifts. A narrow resonance at 5 ppm, similar to that observed for water (D_2O), originates from a small amount of water in the sample, most likely physisorbed to the goethite surface.

Point of Zero Charge of Goethite. Adsorption of ions on the surface of goethite is strongly correlated with the surface charge. The latter can be investigated by measuring the PZC, the PZC value representing the pH value at which the overall

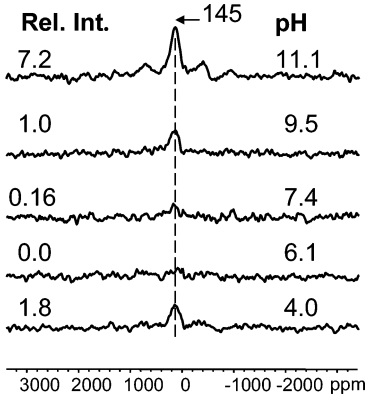

Figure 4. ^{6}Li MAS NMR spectra of Li^{+} adsorbed on goethite (n-α-FeOOH) as a function of pH (series A). The pH of solution and relative intensity of the total spectrum is indicated on the left and right, respectively. Spectra were recorded with a spinning speed of 15.8 kHz.

charge of a material suspended in an aqueous solution is zero. For the n-α-FeOOH sample used for ion sorption studies, a PZC of 8.3 (±0.9) was measured, in excellent agreement with values in the literature.[35] Surprisingly, a different PZC of 4.3 ± 0.3 was obtained for n-α-FeOOD, which is far below the PZC values reported in the literature. Kosmulski et al. recently compiled and evaluated PZC measurements of goethite from more than 170 papers. These authors derived a median PZC for goethite of 8.3 ± 0.9, significantly above the value determined for our n-α-FeOOD.[35] Different PZC values are predicted for the predominant goethite surfaces (9.5 and 8.0 for the (110) and (021) surfaces, respectively), by using the MUSIC model.[14,36,37] These values are higher than the value of our deuterated goethite. SEM and TEM images (Figure 2) show no significant differences between the crystal morphology of the two forms, although our particles do not show clear facets, making analysis more difficult. Similar differences in the PZCs of the deuterated vs protonated particles were also seen for micrometer-sized goethite, systems where differences in particle morphologies were observed.[26] We are currently investigating this apparent H/D isotope effect, and the results will be reported elsewhere. All subsequent sorption and ion-exchange experiments are performed on *protonated* samples of goethite with "normal" PZCs, allowing ready comparison with results reported in the literature for goethite.

^{6}Li MAS NMR Spectra of Li^{+} Adsorbed Goethite. Li^{+} sorption on nano-goethite (n-α-FeOOH) as a function of the pH was investigated from pH = 4.0 to 11.1 by solid-state ^{6}Li MAS NMR for two separate series of samples. For the first set of samples, labeled series A, a broad ^{6}Li resonance centered at $\delta \approx 145$ ppm was observed, along with two weak spinning sidebands, the intensities of the resonances increasing as the pH is increased from 7.4 to 11.1 (Figure 4). No signal is observed for the sample ion-exchanged at pH 6.1. The PZC of this sample (8.3) indicates that the goethite sample will be positively charged at this pH, consistent with the lack of Li^{+} sorption for this sample.

A signal is also seen at pH 4.0, which is unexpected due to the positive surface charge at a pH below the PZC. No attempt to monitor the pH of the experiment at the end of the ion-exchange process was made in these preliminary experiments, and it is possible that an increase in pH value occurred during the sorption experiment, leading to the unexpected result. To test this hypothesis, a new set of samples were prepared (series B), where the pH was monitored both at the beginning and at the end of the sorption experiment. Additional care was taken to remove as much of the ion-exchange solution as possible before air-drying. Now, only a very weak ^{6}Li NMR signal could be detected for the pH 4.0 sample (4.0B), even after 300 000 scans (Figure 5a), as expected on the basis of the PZC. The source of the Li signal in sample 4.0A is not clear, but it may be caused by Li^{+} precipitation during the isolation and drying of the sample. Sample 11.1B (Figure 5c) shows a single, broad resonance with $\delta_{iso}(^{6}Li) \approx 140$ ppm in agreement with the results obtained from series A above the PZC. For the 9.3B sample, the ^{6}Li resonance is asymmetric with a maximum intensity at 55 ppm, with a long tail toward higher ppm values (Figure 5b). This suggests the presence of two or more adsorbed lithium species on the goethite surface, whose concentrations depend on the charge of the goethite nanoparticles.

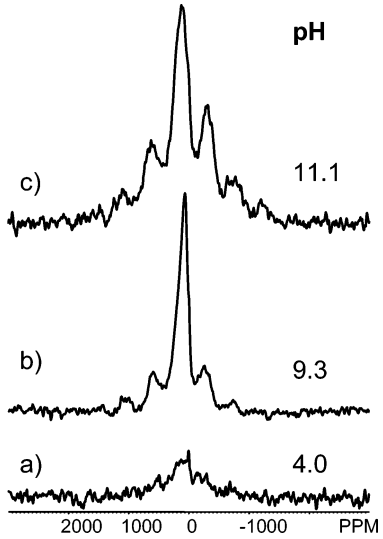

Figure 5. ^{6}Li MAS NMR spectra of Li^{+} adsorbed goethite (n-α-FeOOH; series B). The pH of the solution was (a) 4.0, (b) 9.3, and (c) 10.5. Spectra were recorded with a spinning speed of 14.8 kHz.

Li^{+} Exchange of Micrometer-Sized Goethite Particles. To ensure that the ^{6}Li resonances observed for the ion-exchanged samples are due to Li^{+} ions on the surface of goethite and are not due to ions exchanged for the protons in the goethite tunnels, a Li^{+}-exchanged sample was then investigated by NMR spectroscopy. Since the exchanged sample was prepared from the micrometer-sized goethite, this decreases the ratio of the surface to the bulk, and fewer Li^{+} surface sites are expected. The VT ^{6}Li MAS NMR spectra recorded below 120 °C show a resonance at 0 ppm with two spinning sidebands superimposed on a broad (≈100 kHz), featureless resonance (Figure 6a,b). At this temperature, a second manifold of spinning sidebands with $\delta_{iso} = 289$ ppm appears, as illustrated in Figure 6c. The intensity of this resonance increases on further heating of the sample, while that of the broad resonance diminishes, indicating that the two resonances are related. This phenomenon is identical to that observed in the ^{2}H MAS NMR spectra of m-α-FeOOD,[26] where a broad resonance was observed below T_N (≈120−130 °C), which transforms into a much sharper resonance above this temperature. Thus, the resonance at 289 ppm, which has an identical temperature dependence, is assigned to lithium located inside the 2 × 1 tunnels of the parent goethite structure. The large Fermi contact shift corroborates this assignment. Moreover, no discernible temperature dependence is observed for the isotropic chemical shift in the temperature range of 120−200 °C, indicating the presence of residual anti-ferromagnetism, as also observed in the VT ^{2}H MAS NMR spectra of m-α-FeOOD (vide supra).[26] Li^{+} exchange appears to have negligible effects on T_N.

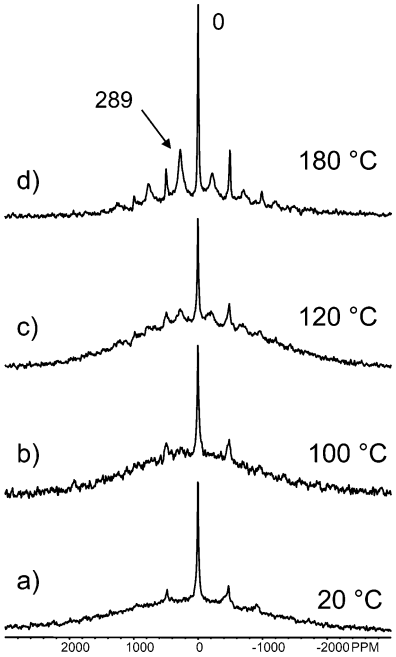

Figure 6. VT ^{6}Li MAS NMR of Li-exchanged goethite as a function of temperature. The isotropic shift of ^{6}Li localized in the tunnels of the goethite structure ($\delta = 289$ ppm) is marked. The peak at $\approx$0 ppm originates from a diamagnetic impurity, most likely residual LiOH or Li_2CO_3. Spectra were recorded with a spinning speed of 14.5 kHz.

The intensity and the position of the resonance at 0 ppm is unaffected by variations in temperature. A 1:1 ratio of LiOH and goethite were employed in the synthesis. Thus, the diamagnetic peak most likely originates from unreacted LiOH or other diamagnetic materials such as Li_2CO_3, due to incomplete ion exchange, a phenomenon observed previously.[31,38] The inefficient exchange of the protons is probably caused by the steric difficulties associated with exchanging ions located inside the one-dimensional 2×1 tunnel system in goethite; most likely, only ions close to the surface are exchanged.

Structural Implications from the ^{6}Li NMR Data. The spectra from both the Li-sorbed and Li-exchanged goethite samples contain resonances with very large shifts. These shifts are well outside the range observed for diamagnetic materials, where shifts of no more than 0 ± 4 ppm are expected. These shifts are ascribed to the through-bond, Fermi-contact shift mechanism,[26] caused by the transfer of unpaired spin density from the Fe^{3+} ions, via the intervening oxygen atoms, to the Li^+ ions. The large Fermi-contact shifts of the main resonances, seen for Li sorption at pH 7.4 and above at approximately 55 and 140 ppm, provide clear evidence for Li−O−Fe bond formation, i.e., in an inner-sphere complex. Generally, the larger the Fermi-contact shift, the larger the number of paramagnetic ions coordinated to the Li^+ ions via the intervening oxygen atoms. Thus, larger shifts will originate from either a lithium species connected to surface oxygen ions coordinated to two or more Fe^{3+} ions and/or from a bidentate or tridentate lithium surface complex. The dominating species at lower pH (55 ppm) most likely has fewer Fe−O contacts than the species seen at higher pH (with an associated resonance at 140 ppm), based on the smaller Fermi-contact shift. However, the fairly broad line width (fwhm = 5.6 kHz) observed for Li^+ adsorbed on goethite at all pH values is somewhat larger than observed for Li-exchanged goethite (3 kHz), reflecting a dispersion in hyperfine shifts due to different sorption sites and/or a variation in the magnetic properties of the individual goethite particles.

The intensity of the ^{6}Li NMR signal due to the Li surface sites increases as the pH increases (Figures 4 and 5) in agreement with the general behavior for sorption on goethite of a variety of metal cations such as Ni^{2+}, Zn^{2+}, Cu^{2+}, and Cd^{2+}; i.e., as the pH increases more metal cations are strongly adsorbed.[39] The (110) ($\approx$90%) and (210) ($\approx$10%) surfaces predominate for high surface area goethite.[11] Venema et al. estimated a PZC for the (110) and (021) surfaces of 9.5 and 8,[37] respectively, with the MUSIC model.[14,36,37,40] These PZCs were calculated by assuming that "Fe_3O" and "FeOH" O sites are the reactive surface sites on the (110) surface. On a (021) surface, oxygen atoms coordinated to one and two Fe atoms prevail.[37] Considering only the species of the dominating (110) surface, a lithium bound to a single FeOH O atom is expected to have a smaller Fermi-contact shift than one bound to an Fe_3O O atom. The "FeOH" binding site is predicted to have a lower PZC than the Fe_3O site,[37] thereby becoming available for Li absorption at a lower pH values. This could account for the observation of a site with a small hyperfine shift at low pH, and a second site with a larger hyperfine shift being seen at higher pH. As the pH is increased, more oxygen sites become deprotonated and sites for Li^+ involving coordination to two or more oxygen atoms may become available, also accounting for the larger hyperfine shift seen for the site occupied by Li^+ at higher pH.

Larger shifts are seen for the resonances assigned to Li^+ in the goethite tunnels. The exact position and bonding arrangement of lithium in the tunnels is unknown, as a detailed crystal structure has not, to our knowledge, been reported. But, based on the similar diffraction patterns seen before and after ion-exchange, the tunnel structure of lithium-exchanged goethite is expected to be similar to that of the proton-exchanged form.[31] The goethite tunnels contain both octahedral and tetrahedral sites, which are both, in principle, available for occupation by lithium. Given a shift of 285 ppm for this tunnel site, it is possible to speculate on the possible binding site for Li, by using approaches similar to those used before for lithium manganates.[29] ^{6}Li hyperfine shifts in the range of 471−543 ppm were observed for lithium in two $LiFeO_2$ polymorphs (α and β).[41] The Li sites in these partially ordered rock-salt compounds are octahedrally coordinated, and contain eight Fe^{3+} ions in the first cation coordination shell and two in the second cation coordination shell with a total of 20 Li−O−Fe bonds. Li^+ ions were placed in the octahedral and tetrahedral sites in the tunnels of goethite, and the numbers of Li−O−Fe bonds were counted. A Li^+ in the tetrahedral tunnel site is connected to the nearby Fe^{3+} ions via 12 Li−O−Fe bonds, while a Li^+ in the octahedral tunnel site is connected to the Fe^{3+} ions via 18 Li−O−Fe bonds. We therefore tentatively assign the ^{6}Li resonance at 285 ppm to the tetrahedrally coordinated lithium, since it contains fewer Li−O−Fe connectivities. The even smaller shifts seen for the surface sites are consistent with even fewer Li−O−Fe connectivities. Studies of a wider range of lithium ferrates are currently underway so as to improve our understanding of the shift mechanisms in these systems. In particular, the effect of the Li−O−Fe bond angles and residual antiferromagnetic correlations between the Fe^{3+} spins on the overall shifts still needs to be determined, to help improve the level of structural detail that can be extracted from the hyperfine shifts.

Conclusions

Nanoparticles of goethite were prepared with particle sizes of 4−10 nm. These particles have lower Néel temperatures than the bulk material and are paramagnetic at room temperature, allowing high-resolution ^{2}H MAS NMR spectra to be obtained.

Li sorption on these particles was investigated, and ^{6}Li NMR signals from Li^+ adsorbed to the goethite surface could be detected even at millimolar concentrations. The ^{6}Li signal intensity increases as the pH of the electrolyte increases, which is consistent with the sorption capacity of goethite for various metal cations reported in the literature. Multiple binding sites for lithium are observed. A resonance at 55 ppm is seen following sorption at a pH of 7.4, the resonance shifting to 145 ppm at higher pH. The shifts seen at close to neutral and high pH are consistent with the formation of a Li^+ inner-sphere complex on the goethite surface, larger shifts indicating tighter binding to more oxygen atoms and/or oxygen atoms coordinated to more Fe^{3+} ions. The possibility that any of these sites arise from Li intercalation in the goethite tunnels was excluded by preparing and obtaining the ^{6}Li spectra of a sample of Li-ion-exchanged goethite.

The work illustrates that solid-state NMR can be used to probe sorption on *paramagnetic* iron−oxyhydroxides nanoparticles. The Fermi-contact shift mechanism can be used to obtain structural information and to distinguish between outer- and inner-sphere binding. The short relaxation times caused by paramagnetic Fe^{3+} ions allows short recycle delays to be used and spectra to be obtained in relatively short periods of time, even for low concentrations of surface sites. The results suggest that it will be feasible to use MAS NMR techniques to study sorption of toxic metal cations and oxyanions, such as Cd^{2+}, Cs^+, $Pb^{2+/4+}$, and SeO_4^{2-} on paramagnetic iron-containing soil minerals.

Acknowledgment. The Center for Environmental Molecular Science is funded by the NSF (Grant CHE-0221934). We thank Danielle Nest for assistance with the PZC measurements. U.G.N. acknowledges the Camille and Henry Dreyfus Postdoctoral Program in Environmental Chemistry and Carlsbergfondet (Grant ANS-1323/20) for financial support.

References and Notes

(1) Brummer, G. W.; Gerth, J.; Tiller, K. G. *J. Soil Sci.* **1988**, *39*, 37−52.

(2) Coughlin, B. R.; Stone, A. T. *Environ. Sci. Technol.* **1995**, *29*, 2445−2455.

(3) Sparks, D. L.; Scheidegger, A. M.; Strawn, D. G.; Scheckle, K. G. *Mineral−Water Interfacial Reactions*; American Chemical Society: Washington, DC, 1998.

(4) Peak, D.; Ford, R. G.; Sparks, D. L. *J. Colloid Interface Sci.* **1999**, *218*, 289−299.

(5) Peak, D.; L., S. D. *Environ. Sci. Technol.* **2002**, *36*, 1460−1466.

(6) Dixit, S.; Hering, J. G. *Environ. Sci. Technol.* **2003**, *37*, 4182−4189.

(7) Schwertmann, U.; Cambier, P.; Murad, E. *Clays Clay Miner.* **1985**, 369.

(8) Schwertmann, U. *Clay Miner.* **1984**, *19*, 9−19.

(9) Schulze, D. G. *Clays Clay Miner.* **1984**, *32*, 36−42.

(10) Schulze, D. G.; Schwertmann, U. *Clay Miner.* **1984**, *19*, 521−539.

(11) Kosmulski, M.; Durand-Vidal, S.; Maczka, E.; Rosenholm, J. B. *J. Colloid Interface Sci.* **2004**, *271*, 261−269.

(12) Elzinga, E. J.; Peak, D.; Sparks, D. L. *Geochim. Cosmochim. Acta* **2001**, *65*, 2219−2230.

(13) Sparks, D. L.; Grundi, T. J. *Mineral−Water Interfacial Reactions: Kinetics and Mechanisms*; American Chemical Society: Washington, DC, 1998.

(14) Hiemstra, T.; Venema, P.; Riemsdijk, W. H. V. *J. Colloid Interface Sci.* **1996**, *184*, 680−692.

(15) Ostergren, J. D.; Brown, J.; Gordon, E.; Parks, G. A.; Persson, P. *J. Colloid Interface Sci.* **2000**, *225*, 483−493.

(16) Hoppe, W. *Z. Kristallogr.* **1940**, *103*, 73−89.

(17) Forsyth, J. B.; Hedley, I. G.; Johnson, C. E. *J. Phys. C* **1968**, *1*, 179−188.

(18) Özdemir, Ö.; Dunlop, D. J. *Geophys. Res. Lett.* **1996**, *23*, 921−924.

(19) Murad, E. *Am. Miner.* **1982**, *67*, 1007−1011.

(20) van der Kraan, A. M.; van Loef, J. J. *Phys. Lett.* **1966**, *20*, 614.

(21) Bocquet, S.; Kennedy, S. J. *J. Magn. Magn. Mater.* **1992**, *109*, 260−264.

(22) Murad, E.; Schwertmann, U. *Clay Miner.* **1983**, *18*, 301.

(23) Kilcoyne, S. H.; Ritter, C. *Physica B* **1997**, *234−236*, 620−621.

(24) Mathé, P.-E.; Rochette, P.; Vandamme, D.; Gérard, F. *Geophys. Res. Lett.* **1999**, *26*, 2125−2128.

(25) Gossuin, Y.; Colet, J.-M.; Roch, A.; Muller, R. N.; Gillis, P. *J. Magn. Reson.* **2002**, *157*, 132−136.

(26) Cole, K. E.; Paik, Y.; Reeder, R. J.; Schoonen, M.; Grey, C. P. *J. Phys. Chem. B* **2004**, *108*, 6938−6940.

(27) Nielsen, U. G.; Skibsted, J.; Jakobsen, H. J. *Chem. Phys. Lett.* **2002**, *356*, 73−78.

(28) Paik, Y.; Osegovic, J. P.; Wang, F.; Bowden, W.; Grey, C. P. *J. Am. Chem. Soc.* **2001**, *123*, 9367−9377.

(29) Grey, C. P.; Lee, Y. J. *Solid State Sci.* **2003**, *5*, 883−894.

(30) Goodmann, B. A.; Lewis, D. G. *J. Soil Sci.* **1981**, *32*, 351−363.

(31) Sakurai, Y.; Arai, H.; Okada, S.; Yamaki, J.-I. *J. Power Sources* **1997**, *68*, 711−715.

(32) Miller, J. F.; Schatzel, K.; Vincent, B. *J. Colloid Interface Sci.* **1991**, *143*, 532−554.

(33) Miller, J. F.; Velev, O.; Wu, S. C. C.; Ploehn, H. J. *J. Colloid Interface Sci.* **1995**, *174*, 490−499.

(34) Goodenough, J. B. *Magnetism and the Chemical Bond;* John Wiley & Sons: New York, 1963.

(35) Kosmulski, M.; Maczka, E.; Jartych, E.; Rosenholm, J. B. *Adv. Colloid Interface Sci.* **2003**, *103*, 57−76.

(36) Hiemstra, T.; de Witt, J. C. M.; van Riemsdijk, W. H. *J. Colloid Interface Sci.* **1989**, *133*, 105−117.

(37) Venema, P.; Hiemstra, T.; Weidler, P. G.; van Riemsdijk, W. H. *J. Colloid Interface Sci.* **1998**, *198*, 282−295.

(38) Matsumara, T.; Kanno, R.; Inaba, Y.; Kawamoto, Y.; Takano, M. *J. Electrochem. Soc.* **2002**, *149*, A1509−A1513.

(39) Langmuir, D. *Aqueous Environmental Geochemistry*; Prentice Hall: Saddle River, NJ, 1997.

(40) Hiemstra, T.; van Riemsdijk, W. H. *J. Colloid Interface Sci.* **1996**, *179*, 488−508.

(41) Pan, C. Li NMR Studies of $LiMO_2$. M.Sc. Thesis, SUNY Stony Brook, NY, 2000.